International Symposium on Space Flight Dynamics

ORBIT DETERMINATION AND NAVIGATION OF THE SOLAR TERRESTRIAL RELATIONS OBSERVATORY (STEREO)[1]

Michael Mesarch & Mika Robertson (GSFC)
Neil Ottenstein, Ann Nicholson, Mark Nicholson, & Douglas T. Ward (a.i. solutions, Inc.)
Jennifer Cosgrove, Darla German, & Stephen Hendry, James Shaw (HTSI)

Abstract

This paper provides an overview of the required upgrades necessary for navigation of NASA's twin heliocentric science missions, Solar TErestrial RElations Observatory (STEREO) Ahead and Behind. The orbit determination of the STEREO spacecraft was provided by the NASA Goddard Space Flight Center's (GSFC) Flight Dynamics Facility (FDF) in support of the mission operations activities performed by the Johns Hopkins University Applied Physics Laboratory (APL). The changes to FDF's orbit determination software included modeling upgrades as well as modifications required to process the Deep Space Network X-band tracking data used for STEREO. Orbit results as well as comparisons to independently computed solutions are also included. The successful orbit determination support aided in maneuvering the STEREO spacecraft, launched on October 26, 2006 (00:52 Z), to target the lunar gravity assists required to place the spacecraft into their final heliocentric drift-away orbits where they are providing stereo imaging of the Sun.

1. Introduction

The twin STEREO spacecraft were successfully launched on October 26, 2006, at 00:52 Z on a Delta-II 2925 launch vehicle from the Cape Canaveral Air Force Station. STEREO-A (Ahead) and STEREO-B (Behind) reached their mission orbits on December 15, 2006, and January 21, 2007, respectively. The NASA Goddard Space Flight Center (GSFC) Flight Dynamics Facility (FDF) is providing orbit determination and navigation support services for the STEREO spacecraft in a collaborative role with the mission lead center and mission design team from the Johns Hopkins University Applied Physics Laboratory (APL). Reference 1 provides an overview and history to the STEREO Mission.

The STEREO spacecraft are in leading (Ahead) and lagging (Behind) heliocentric drift-away orbits, moving away from the Earth at ±22 degrees/year. The mission orbits were achieved using a phasing loop transfer to a lunar gravity assist as was done for the FDF supported Wilkinson Microwave Anisotropy Probe (WMAP) mission in 2001. Further FDF experience in this orbit regime includes support for at least 36 lunar gravity assists for the Interplanetary Physics Laboratory spacecraft (better known as Wind) mission since its launch in 1994.

Tracking support for these spacecraft is provided by NASA's Deep Space Network (DSN) X-band antennas, which use variable frequencies during spacecraft ranging. Upgrades in the Goddard Trajectory Determination System (GTDS) orbit determination and prediction software were necessary for support of the spacecraft. These upgrades included changes to the dynamic force modeling capabilities, relativistic modeling, and heliocentric modeling, as well as the implementation of new range and Doppler measurement models necessary for navigation support using the Deep Space Network (DSN) X-band service. Following the software changes, testing was performed using a small set of data with orbit characteristics similar to the STEREO orbit regimes. The satellite data used for testing was obtained from the Mars Reconnaissance Orbiter (MRO), Stardust, and Deep Impact missions. Furthermore, funding was obtained to perform an independent assessment of the STEREO orbit determination by the Jet Propulsion Laboratory's (JPL) Multi-Mission Navigation team. Key orbit solutions were obtained in an effort to further validate the GTDS upgrades. The solutions identified as being important included deliveries to APL at launch plus 24 hours (L+24h), prior to first perigee, and prior to fourth perigee. The L+24h orbit solution represented the first solution suitable for maneuver planning. The first and fourth perigee solutions were longer arcs (3 to 5 days) and important in case maneuvers were needed at the respective perigees.

Orbit Determination Requirements

The STEREO orbit determination (OD) accuracy requirements are associated with support of onboard attitude processing, reduction of scientific measurements, and also detailed maneuver planning. The required accuracies

[1] This paper was supported by the National Aeronautics and Space Administration (NASA)/Goddard Space Flight Center (GSFC), Greenbelt, MD, under MOMS contract (NNG04DA01C), Task Orders #109 and #28

were different for the three major phases of operations – early orbit (first 24 hours), the phasing loops, and the heliocentric mission orbit. While the requirements during the first 24 hours were "best effort," the need for high precision in the orbit estimation was especially acute during the lunar phasing loop periods for planning and targeting the proper lunar gravity assists by the mission design team. The expected orbital accuracies based on pre-mission error analysis[2,3] and the required orbital accuracies for each mission phase are presented below in Table 1.

For the phasing loops phase prior to STEREO's gravity assist, the orbit determination requirements are 9.4 km accuracy around the fourth perigee, necessary to properly target the required mission orbit drift rate achieved via a lunar gravity assist. In the heliocentric mission orbit, the orbit determination requirements for science are 7500 km (3σ) predicted accuracy over 30 days.

Table 1. STEREO Orbit Determination and Prediction Requirements and Pre-mission Expected Accuracies

	First 24 Hours	Phasing Loops	Heliocentric Mission Orbit
Definitive Requirements	Best available	9.4 km 2.7 cm/sec at P4	N/A
Predictive Requirements	Best available	Best available	7500 km over 30 days
Pre-mission Expected Accuracy	24 hrs: 844 m definitive 1.5 km predicted to 48hr	1-2 km definitive knowledge using 5 day solution arcs	First 7 days after lunar gravity assist: 1.3 km definitive 14-day definitive: 6.95 km @ 1-year, 14 day solutions definitive: 114 km @ 1-year, 30 day solutions definitive: 89 km

The results presented in this paper span from the ascent trajectory phase, which includes launch, the trans-lunar phasing loops, to the lunar gravity assists, and the mission orbit phase. Also included are the comparisons to the results provided by JPL. Early operations experience and mission design decisions and implementation from the APL point of view are provided in References 2 through 5.

2. FDF Software Upgrades

DSN provides X-band TRK 2-34 range and Doppler tracking data types for the STEREO spacecraft. The STEREO X-band TRK 2-34 range data is different from the TRK 2-34 range data previously processed in the FDF because for STEREO the DSN trackers employ linearly varying transmit frequencies. This section describes the modifications that were needed to the FDF software to process the STEREO range data.

Tracking Data Definition

Compensation of uplink frequency to cancel predicted Doppler shift at the spacecraft receiver is a standard practice, when required by the narrowness of the spacecraft receiver bandwidth or the vulnerability of the signal waveform to distortion. DSN tracking of the STEREO spacecraft is an example of the first situation, while Tracking and Data Relay Satellite (TDRS) users, with pseudo-noise (PN) coded signals, are examples of the second situation. The DSN implementation of Doppler compensation uses a discrete set of predicted Doppler compensated transmit frequencies and their associated times of transmission. The actual transmit frequency at a given time is linearly interpolated from the frequencies nearest in time in the discrete set. It is a STEREO mission requirement that the DSN trackers implement Doppler compensation by the use of "ramped" frequencies.

The STEREO mission uses X-band transponders on both spacecraft and is supported by the DSN using DSN TRK-2-34 data. The TRK-2-34 data specification (Ref. 6) contains a number of data types. The data types of interest for STEREO are Type 7 data, which is sequential range data (Ref. 7), Type 17 data, which is total phase observable, and Type 9 data, which is ramp report data. Doppler data is derived from type 17 data.

---

[2] J. Lorah, *Follow-On Analysis of Orbit Determination Accuracies During the Solar Terrestrial Relations Observatory (STEREO) Phasing Loop Mission Phase*, FDF-109-011, Honeywell Technology Solutions Inc., March 22, 2006.

[3] L. Chung and T. Lee, *Solar Terrestrial Relations Observatory (STEREO) Mission Orbit Study*, FDF-109-017, Honeywell Technology Solutions Inc., September 22, 2006.

The ramp report data contains the uplink frequency, f_R, at the start of the ramp, the timestamp at the start of the ramp, t_R, and the ramp rate, f_Δ, which is the slope of the linear ramp. The transmit frequency at an intermediate time, *t*, during the ramp period can be found as:

$$F_T(t) = f_R + f_\Delta \cdot (t - t_R) \tag{1}$$

The complexity in the processing of observed ramped frequency range and range-rate (Doppler) data arises from the necessity to light-time correct the times used in the frequency calculation of the transmission frequency. This leads to the situation in which accurate round trip light-time (RTLT) values are needed to convert the raw range from range units to range in meters is itself a measurement of RTLT. The problem and solution are described in detail in the following sections.

Description of Problem

The DSN trackers, when not using a fixed transmit frequency, ramp the frequency at a constant slope between discrete, instantaneous changes in slope. A "ramp report" message is sent out with each change in slope. The challenge, since the frequency is dynamic, is that the RTLT must be known accurately to correctly convert the range measurement, which is explicitly a measurement of RTLT. If t_{rt} is the RTLT, and the range measurement is being made at time t_M, then the transmit frequency in use at the time the observed ranging waveform was transmitted is:

$$F_T(t_M - t_{rt}) = f_R + f_\Delta \cdot (t_M - t_{rt} - t_R) \tag{2}$$

However, t_{rt} is the desired measurement, and is thus not actually known, and must be estimated from an *a priori* orbit ephemeris.

Conversion to Observed Range

For the ramped frequency case, the observed value of the two-way ramped sequential ranging assembly range observable, ρ_{RU}, is given by

$$\rho_{RU} = \frac{221}{1498} \int_{t_{T_{Up}}}^{t_{R_{Down}}} F_T(t)\, dt, \quad \text{modulo M (RUs)} \tag{3}$$

and the equivalent ambiguous 2-way range measurement in kilometers, ρ, is given by

$$\rho = \frac{1498}{221} \frac{c\ \rho_{RU}}{\frac{1}{t_{rt}} \int_{t_{T_{Up}}}^{t_{R_{Down}}} F_T(t)\, dt} \tag{4}$$

where

RU is the range count from the raw data.

M is the length of the ranging code in range units (RUs).

c is the speed of light.

F_T is the transmit frequency in Hz.

$t_{R_{Down}}$ is the reception time.

$t_{T_{Up}}$ is the transmission time from the ground station.

This integral is evaluated using the ramped frequency records following the procedure given in Section 13.3.2.2.2 in Reference 8. For the simple case where the entire integration time interval is within one ramp record, the integral equals the average transmission frequency over the light time multiplied by the RTLT.

For the unramped frequency case, the transmission frequency is a constant and the above equations reduce to

$$\rho_{RU} = \frac{221}{1498} F_T t_{rt}, \quad \text{modulo M (RUs)} \tag{5}$$

The corresponding ambiguous range is given by

$$\rho = \frac{1498}{221} \frac{c}{F_T} \rho_{RU} \tag{6}$$

Conversion to Observed Range-rate

For the DSN TRK-2-34 format, the raw data is a count of cycles of the return carrier frequency. The cumulative Doppler count, C(t), is as follows, where K is the coherent turn-around ratio (K = 240/221 for S-band, and K = 880/749 for X-band).

$$C(t) = C(t_0) + \int_{t_0}^{t} f_R(s)ds = C(t_0) + K \int_{t_0 - \frac{2}{c}\rho(t_0)}^{t - \frac{2}{c}\rho(t)} F_T(h)dh \tag{7}$$

The differenced Doppler count (DC), where τ ($t - t_0$) is the Doppler count interval (DCI), is

$$DC(t) = K \int_{t-\tau-\frac{2}{c}\rho(t-\tau)}^{t-\frac{2}{c}\rho(t)} F_T(h)dh \tag{8}$$

This relationship is inverted to obtain the average range-rate over the DCI.

Since the average frequency over the DCI is

$$\overline{F}_T = \frac{1}{t - \frac{2}{c}\rho(t) - \left(t - \tau - \frac{2}{c}\rho(t-\tau)\right)} \int_{t-\tau-\frac{2}{c}\rho(t-\tau)}^{t-\frac{2}{c}\rho(t)} F_T(h)dh, \tag{9}$$

$DC(t)$ can be written as

$$\begin{aligned} DC(t) &= K\overline{F}_T \left[t - \frac{2}{c}\rho(t) - \left(t - \tau - \frac{2}{c}\rho(t-\tau) \right) \right] \\ &= K\overline{F}_T \left[\tau - \frac{2}{c}\left(\rho(t) - \rho(t-\tau)\right) \right] \\ &= \tau K \overline{F}_T \left[1 - \frac{2}{c}\dot{\rho}(t) \right] \end{aligned} \tag{10}$$

Finally, the average range-rate, ρ(t), is

$$\overline{\dot{\rho}}(t) = \frac{c}{2}\left(1 - \frac{DC(t)}{\tau K \overline{F}_T} \right) \tag{11}$$

FDF Tracking Data Flow

In the FDF implementation, raw tracking data enters through the NASCOM Front End Processor (NFEP). The DSN Type 7 (range), 9 (ramp report), and 17 (Doppler) data are converted to the required units and format by the Tracking Data Formatter (TDF) program, and then written to an ORACLE database by the database loader programs. The Presenter program retrieves data from the database according to user-specified criteria and writes an OD input file known as the 60-byte file. For a variable ramp data set (i.e., a data set with non-zero ramp rate in the Type 9 data ramp reports), this 60-byte file contains range data, range-rate data, and ramp report data formatted for use by the Goddard Trajectory Determination System (GTDS) program, which performs the OD.

The STEREO modifications to the observation processing programs are as follows. The range and range-rate observations are converted from raw units in TDF using the frequency contained in the most recent ramp report (Type 9 data). Thus the data written to the database by the loader programs is uncorrected for variable frequency at the observation time. The Presenter program retrieves the uncorrected data from the database and writes a 60-byte file containing the range data, the range-rate data, and the complete set of ramp reports for the user specified timespan, including timestamp, frequency at the start of the ramp, and ramp rate. The correction for the variable frequency is performed iteratively during the OD processing in GTDS.

Corrections During Orbit Determination

In GTDS, the observations are corrected at each differential correction iteration by using the updated estimate of the range to adjust the frequency. Note that integrals may be calculated over intervals containing multiple ramp reports, in which case the integrals are calculated as for segmented functions.

Initialization of the iteration is:

$$\begin{aligned} &R_0(t) = R_{60}(t), \quad \overline{\dot{R}}_0(t) = \overline{\dot{R}}_{60}(t) \\ &\rho_0(t) = t_{rt}\frac{c}{2} \\ &F_0(t) = f_R 7 \end{aligned} \tag{12}$$

At iteration n, the updates are:

$$\begin{aligned} &F_n(t) = f_R + f_\Delta\left(t - \frac{2}{c}\rho_n(t) - t_R\right) \\ &\overline{F}_n^{DCI}(t) = \frac{1}{t - \frac{2}{c}\rho_n(t) - \left(t - \tau - \frac{2}{c}\rho_n(t-\tau)\right)} \int_{t-\tau-\frac{2}{c}\rho(t-\tau)}^{t-\frac{2}{c}\rho(t)} F(h)dh, \\ &\overline{F}_n^{RTLT}(t) = \frac{1}{t_{rt}} \int_{t_{T_{Up}}}^{t_{R_{Down}}} F_n(t)\,dt \\ &R_n(t) = R_{n-1}(t)\frac{\overline{F}_{n-1}^{RTLT}(t)}{\overline{F}_n^{RTLT}(t)} \\ &\overline{\dot{R}}_n(t) = \overline{\dot{R}}_{n-1}(t)\frac{\overline{F}_{n-1}^{DCI}(t)}{\overline{F}_n^{DCI}(t)} + \frac{c}{2}\left(1 - \frac{\overline{F}_{n-1}^{DCI}(t)}{\overline{F}_n^{DCI}(t)}\right) \end{aligned} \tag{13, 14}$$

where

t is the observation timetag

f_R is the frequency in the applicable ramp report

t_R is the timetag of the applicable ramp report

R_{60} is the range written to the 60 byte file

$\bar{\dot{R}}_{60}$ is the average range rate written to the 60 byte file

$R_n(t), \bar{\dot{R}}_n(t)$ are the corrected observed range and average range rate at time t and iteration n

$F_n(t)$ is the transmit frequency at time t and iteration n

$\bar{F}_n^{DCI}(t)$ is the average frequency at time t over the DCI at iteration n

$\bar{F}_n^{RTLT}(t)$ is the average frequency at time t over the RTLT at iteration n

$\rho_n(t)$ is the computed range at time t and iteration n

Relativistic Corrections

To improve the dynamic modeling used in the OD process, a relativistic point mass acceleration was added [Ref. 9 and 10]

$$\ddot{\bar{r}}_{PM_{rel}} = \frac{\mu_S}{c^2\left(r^P\right)^3}\left[\left(4\frac{\mu_S}{r^P} - \left(v^P\right)^2\right)\bar{r}^P + 4\left(\bar{r}^P \cdot \bar{v}^P\right)\bar{v}^P\right] \tag{15}$$

where

r^P, v^P are position and velocity of the spacecraft with respect to the Sun

μ_S is the gravitational constant of the Sun.

Also to improve the measurement modeling used in the OD process, a relativistic light time correction to the computed range was added [Ref. 8 and 11], resulting in an increase in the computed range on the order of a kilometer. ψ_{21} is a relativistic time delay that accounts for the reduction on the coordinate velocity of light due to the mass of the Sun. When multiplied by the speed of light, ψ_{21} is an additive correction to the computed range. The correction is

$$\psi_{21} = \frac{2\mu_S}{c^3}\ln\left[\frac{r_1 + r_2 + r_{12}}{r_1 + r_2 - r_{12}}\right] \tag{16}$$

where

μ_S is the gravitational constant of the Sun

r_1 is the spacecraft to Sun distance

r_2 is the ground station to Sun distance

r_{12} is the ground station to spacecraft distance

3. Results for STEREO-Ahead and STEREO-Behind Orbit Navigation

Overview

The orbit determination and orbital prediction results are grouped together by mission phase:

- Launch + first 24 hours (Earth-centered trajectory)
- Phasing loops (to final lunar gravity assist, Earth-centered trajectory)
- Heliocentric mission orbits (Sun-centered trajectory)

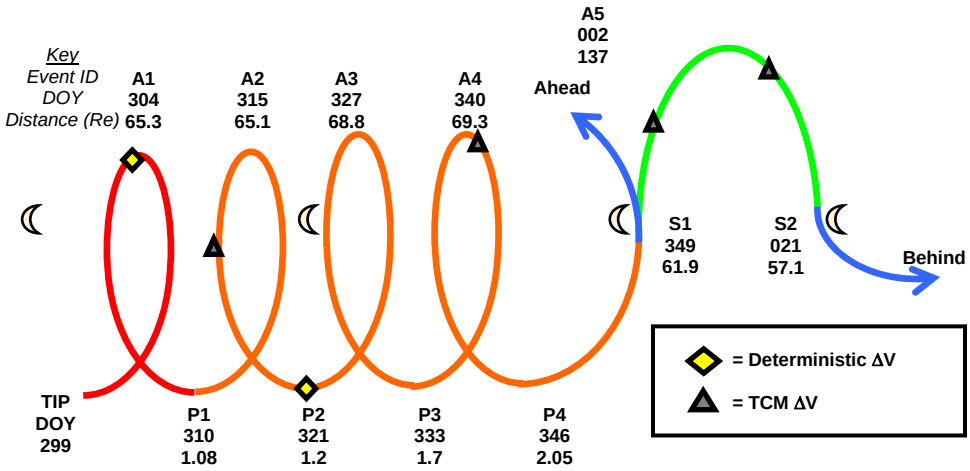

Figure 1. Phasing Loop Schematic

The phasing loop schematic (Figure 1) shows the day of year (DOY) for the targeting interface point (TIP), when each of the apogees (A*x*), perigees (P*x*), and lunar gravity assists (S1 and S2) occurred, and the distance from the center of the Earth in units of Earth radii (1 Earth radius is 6378.14 km). The diagram attempts to present a simplistic view of the phasing loops, the Moon is not near every apogee, but the spacecraft's trajectories are phased correctly to place the spacecraft at the right apogee near to the Moon. At this apogee, the spacecraft are targeted to pass by at the proper distance and angle to provide the correct orbital energy change to send the spacecraft onto their mission trajectories. The distances represented are for Behind's trajectory, although since both were on the same trajectory until the first lunar gravity assist, it is a fair representation of both orbits. Behind had one additional lunar gravity assist beyond Ahead, which sent it onto its final trajectory, away from the Sun. Symbols representing the locations of the various maneuvers conducted during these phases (with the exception of the engineering burns and momentum management burns) are also included.

There were approximately 5 to 6 days between each perigee to apogee passage on the phasing loops to properly position each spacecraft relative to the required lunar encounter or "swingby." The phasing loops were all performed using Earth as the central body.

Spacecraft Orbit Estimation and Force Modeling

Definitive overlap comparisons are used to ascertain orbital consistency or accuracy. The overlap period is defined as the set of tracking data that is common to consecutive solution arcs during the batch least-square orbit determination process. The root-mean-square (RMS) position and velocity differences are measured and recorded (1-sigma results). Predictive accuracy is measured by a similar approach, although a predictive ephemeris is recorded and later compared to a definitive solution of the target predict interval. For the predictive comparisons, the maximum position differences (MPD) are captured (3-sigma). STEREO achieved orbital accuracies are shown in Table 3 and further analysis of the results is presented in Figures 2 through 4.

Table 2 presents a summary of the solution parameters per orbital phase of the mission, including arc length, definitive overlap periods between consecutive solutions, solve-for parameters, force models, integration method and step size, source of planetary ephemeris information, and Earth gravity modeling.

Table 2. STEREO Modeling and Solution Parameters

	Launch Period	Lunar Phasing Loops	Heliocentric
Tracking Data (Goldstone, Madrid, Canberra)	Near continuous	Tracking 12 hr/day transitioning to 3 hr/day	3.5 hours/day
OD Arcs	TIP to end of data arc	5 days (typical)	21-28 days (typical)
Overlapping Arcs	-	2-3 days	14 days
Estimated Parameters	Position, Velocity	Position, Velocity, SRP coefficient, range biases as necessary	Position, Velocity, SRP coefficient, range biases as necessary
Force Models	SRP with spherical area Point mass Sun, Moon, Planets (without Neptune)	SRP with spherical area Point mass Sun, Moon, Planets (without Neptune)	SRP with box-wing model Point mass Sun, Earth, Moon, Planets (without Neptune)
Integration	Cowell, 60 seconds	Cowell, 60 seconds	Cowell, 60 seconds
Planetary Ephemeris	DE 405	DE 405	DE 405
Earth Gravity	JGM-2 Order 20, Degree 20	JGM-2 Order 20, Degree 20	Point mass

Table 3 presents a summary of the collective definitive and predictive accuracies achieved. In addition to the position and velocity vectors, the solar radiation pressure coefficient, C_r, is also estimated. Range biases were also determined as necessary to provide good solutions. During the early orbit and trans-lunar phases of the mission, orbital updates were performed more often to maintain good network coverage during early mission critical deployments, engineering burns, and planning and recovering from the orbital maneuver burns. Perigee passages also provided a large orbital perturbation. Update frequencies were also tied to the maneuver planning process to provide the mission design team the latest navigation results to plan the lunar gravity assist required for transition to the correct mission orbit. As the spacecraft transitioned to the mission orbits, the frequency of these updates was significantly reduced, with updates occurring no more frequently than every 14 days, as expected.

When the spacecraft transitioned to heliocentric from Earth-centered, the solar radiation pressure model was changed from a spherical model to a more complex box-wing model, which better represents the surface area with the change in attitude profile on the Sun-centered mission orbit. Also in the heliocentric orbits, the Earth gravity diminished as a significant perturbation, and the Earth was switched to a point mass representation identical to that used for the other planetary bodies. FDF software limits the number of planetary bodies included in the integration of the equations of motion; therefore Neptune was neglected as a perturbing body.

The definitive accuracies shown in Table 3 demonstrate that for each mission phase the achieved orbital accuracies consistently met requirements (Table 2) and have been well within the pre-mission covariance studies predictions. The launch period results were slightly higher than expected based on pre-mission error analysis. Ahead's definitive solution consistency performance was often half of that achieved on Behind for the Earth-centered phases, although both are well within requirements. For the early orbit period, the average RMS position difference is 1370 meters for Ahead, versus the 2640 meters achieved on Behind. The in-track and radial component differences are larger here than in the better determined phasing loops results. This is an expected result, since the achieved orbit size is the hardest orbital parameter to estimate on short-arc solutions. During this early phase, the solar radiation pressure was mainly applied instead of estimated due to the shorter data arc.

Table 3. STEREO Definitive and Predictive Solution Results

	Launch Period	Lunar Phasing Loops	Heliocentric
Average Definitive Overlap Differences (m) 1-sigma	*Ahead:* R 324 I 957 C 713 Total 1370 *Behind:* R 1020 I 2070 C 1230 Total 2640	*Ahead:* R 17 I 131 C 181 Total 241 *Behind:* R 12 I 164 C 246 Total 321	*Ahead:* R 1160 I 1250 C 1990 Total 2750 *Behind:* R 388 I 782 C 712 Total 1240
Average Parallel Definitive vs. JPL Ephemeris (m)	*Ahead:* R 20 I 98 C 300 Total 434 *Behind:* R 15 I 196 C 199 Total 286	*Ahead:* R 10 I 19 C 174 Total 180 *Behind:* R 16 I 111 C 575 Total 589	Not Available
Average Predictive Error (m) up to 7-14 Days 3-sigma		*Ahead:* R -370 I 374 C -634 Total 1360 *Behind:* R -28 I -163 C -54 Total 657	*Ahead:* R -331 I 21 C -424 Total 6200 *Behind:* R -97 I -419 C -153 Total 2470

Note: R= Radial, I=In-Track, C=Cross-Track

Figures 2 and 3 display the lunar phasing loops definitive overlap difference results for both Ahead and Behind. The maneuvers during this time frame (including engineering burn #2 [E2]) are marked at the top of the figures. Both were quite consistent with the average overlap RMS comparisons of 241 meters for Ahead and 321 meters for Behind. For both spacecraft, the largest component errors were in the cross-track direction.

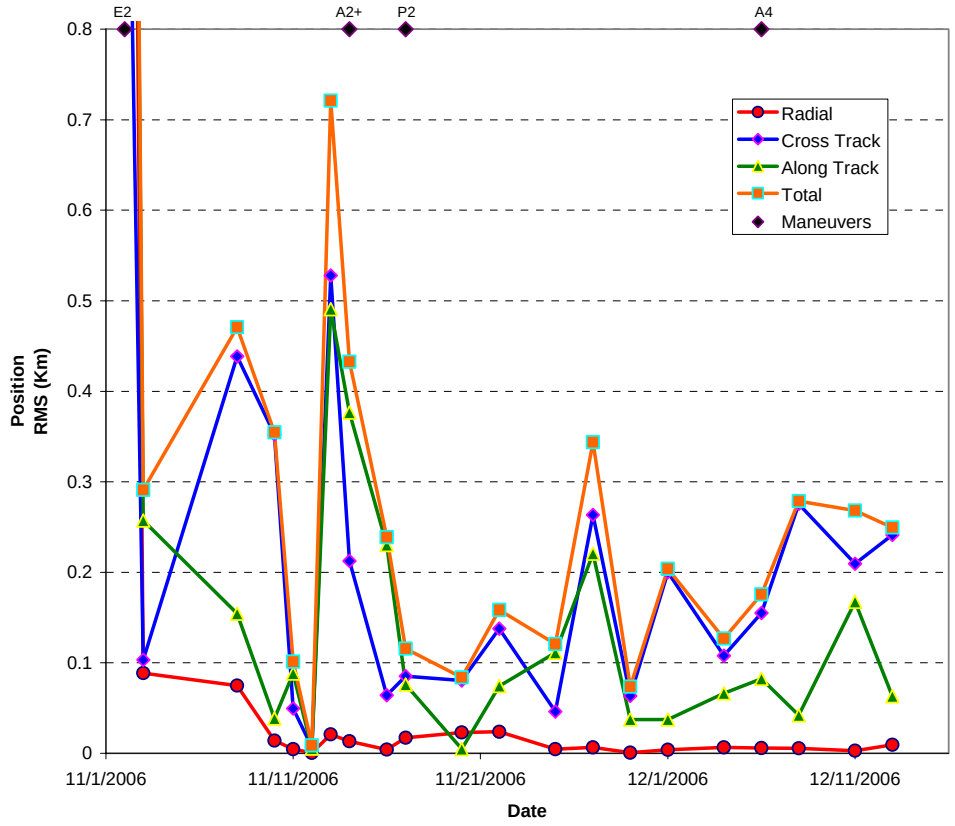

Figure 2. Ahead Definitive Position RMS Overlap Differences During Lunar Phasing Loops

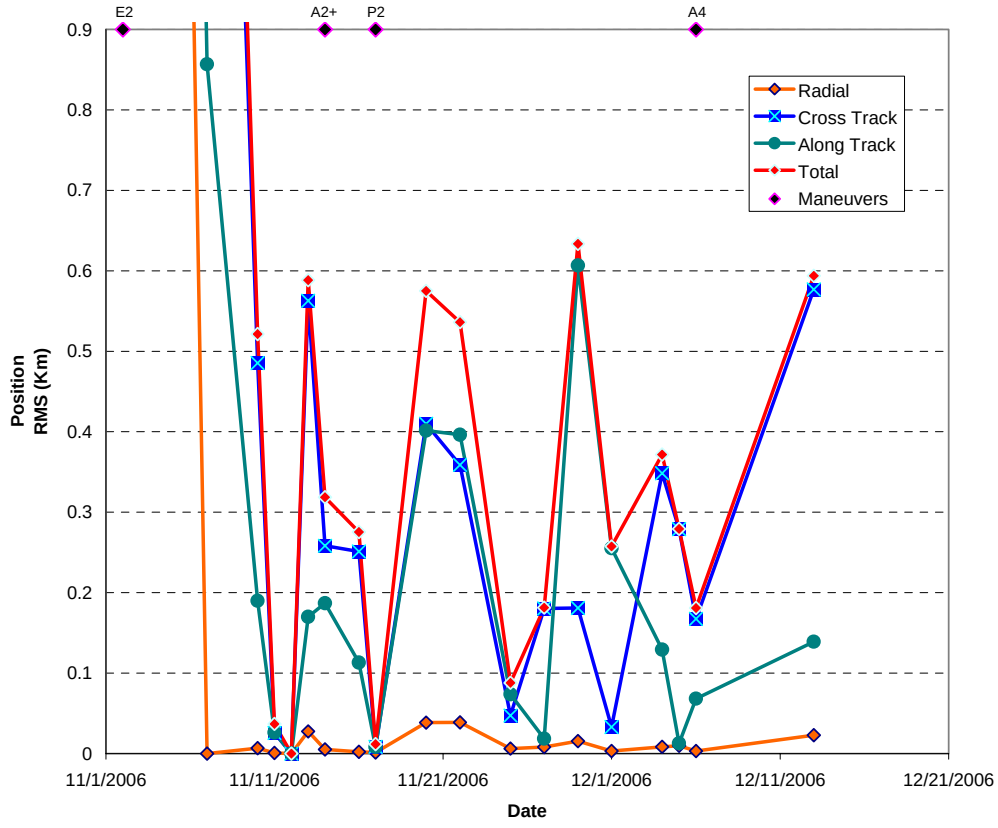

Figure 3. Behind Definitive Position RMS Overlap Differences During Lunar Phasing Loops

Behind's trajectory diverged from Ahead's at the first lunar gravity assist (S1) as planned, with a second encounter with the Moon (for Behind only) (S2) occurring 37 days later. Figure 4 displays the definitive accuracies for the heliocentric phase of each mission. An interesting trend on the plot shows that as the spacecraft travel away from the Earth, the definitive error results continue to increase. At a range of approximately 5 million kilometers from the Earth, the results for Ahead display approximately a 5 km definitive accuracy. If it continues at this rate, at a range of 150 million km, the expected definitive accuracy may be on the order of 150 km, results which are consistent with the pre-mission error analysis results[4]. Pre-mission error covariance analysis performed did not include perturbations from Uranus and Mercury but also neglected Neptune's perturbations, as does the mission navigation. However, Ahead's results are in line with the predictions.

Behind's definitive error is also increasing as a function of range. However, the overall growth rate is only approximately half of the rate of Ahead, generally a reverse of the trend seen in the Earth-centered trajectory phase of the mission. The spacecraft are generally traveling away from the Earth at a rate of approximately 60 million km/yr. Since Ahead is traveling closer to the Sun and Behind is further away from the Sun, the perturbations on the spacecraft are not identical. Perhaps the perturbations on Ahead are modeled less accurately than Behind as both traverse the Solar System. Ahead experiences more gravitational influences from less distant bodies as well as greater solar radiation forces.

At the continuation of the same rate, Behind will also be well within the required accuracies for the duration of the mission life. The 7500-km accuracy requirement over a 30-day predictive period (3-sigma) is to ensure that the HGA points back at the Earth from orbit to enable the communication link correctly[5]. (Note that in the legends of the following plots, Ahead and Behind are abbreviated to STA and STB, respectively.)

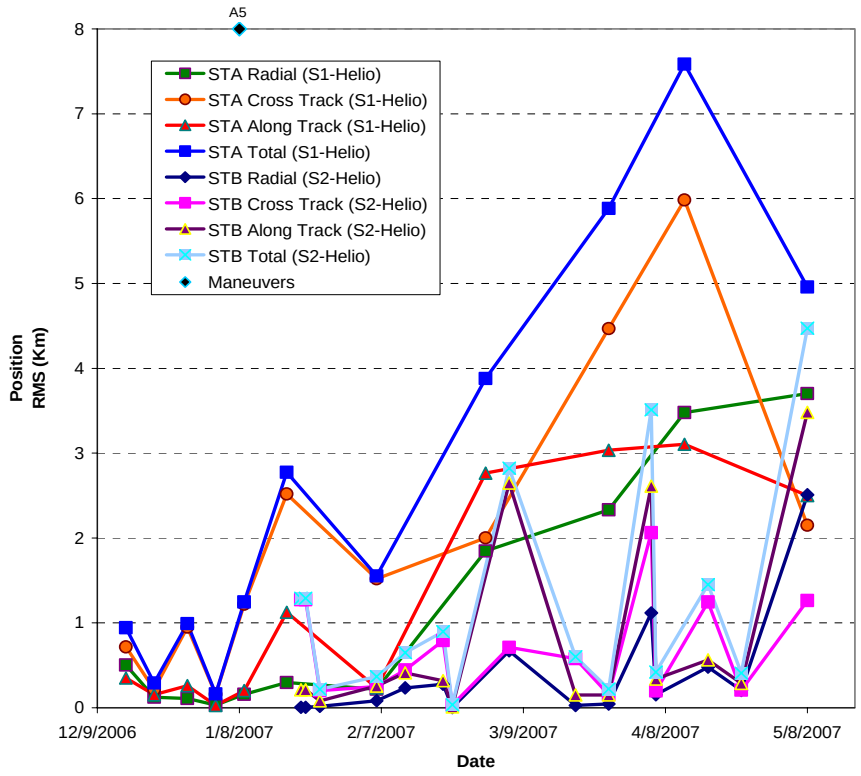

Figure 4. Ahead and Behind Definitive Position RMS During Heliocentric Phase

For ephemeris deliveries through June 6, 2007, the 30-day heliocentric orbit prediction comparisons (with respect to the definitive solutions) were all within 340 km for both Ahead and Behind. Momentum unloads are typically not modeled until after they occur. OD solution data arcs are broken across each momentum unload. Post-maneuver solutions are performed approximately 14 days and 28 days following each unload. The 14-day solutions are

[4] L. Chung and T. Lee, *Solar Terrestrial Relations Observatory (STEREO) Mission Orbit Study*, FDF-109-017, Honeywell Technology Solutions Inc., September 22, 2006

[5] The Johns Hopkins University Applied Physics Laboratory (APL), *Systems Requirements Document (SRD) STEREO*, Revision B, June 21, 2004.

compared to the 28-day solution arcs. Subsequent orbital solutions are performed every 2 weeks. This approach results in solution overlap periods of approximately 14 days in length.

When the predictions just before momentum unloads are excluded, all accuracies were below 190 km. The Behind momentum unloads are smaller and the prediction accuracies for Behind averaged 18 km less than for Ahead. These accuracies are all well below the 7500-km 3-sigma requirement. Pre-launch estimates of the frequency of unload thruster burns to disperse the momentum build-ups assumed worst case frequencies of every 14 days. The observed intervals during the mission have been less often. The unload plan is currently every 6 weeks for Ahead and every 9 weeks for Behind (changed from 6 weeks). This is also further confirmation that the perturbations for Ahead are approximately 50 percent higher on Ahead than Behind as seen from the definitive and predictive error growth rates observed from the estimation results.

Figure 5 shows that C_r values range from 1.2 to 1.4 at the beginning of the mission and then settled to just short of 1.4 for Ahead before the first lunar gravity assist (S1) and then closer to 1.4 for Behind during the outer loop. In the heliocentric phase, the results were about 1.2 for both Ahead and Behind. The solar radiation pressure coefficients generally change more in early mission solution estimates because the solved-for pressure perturbation is hard to determine in early mission due to spacecraft outgassing and short solution arcs especially for the large orbits of the STEREO spacecraft. Stabilization of the solar radiation pressure force occurred within a few days of launch. The transition to the heliocentric phase brought about a desired transition to more complex area modeling, and the resultant solved-for solar pressure coefficient is much more stable at this point with the improved modeling.

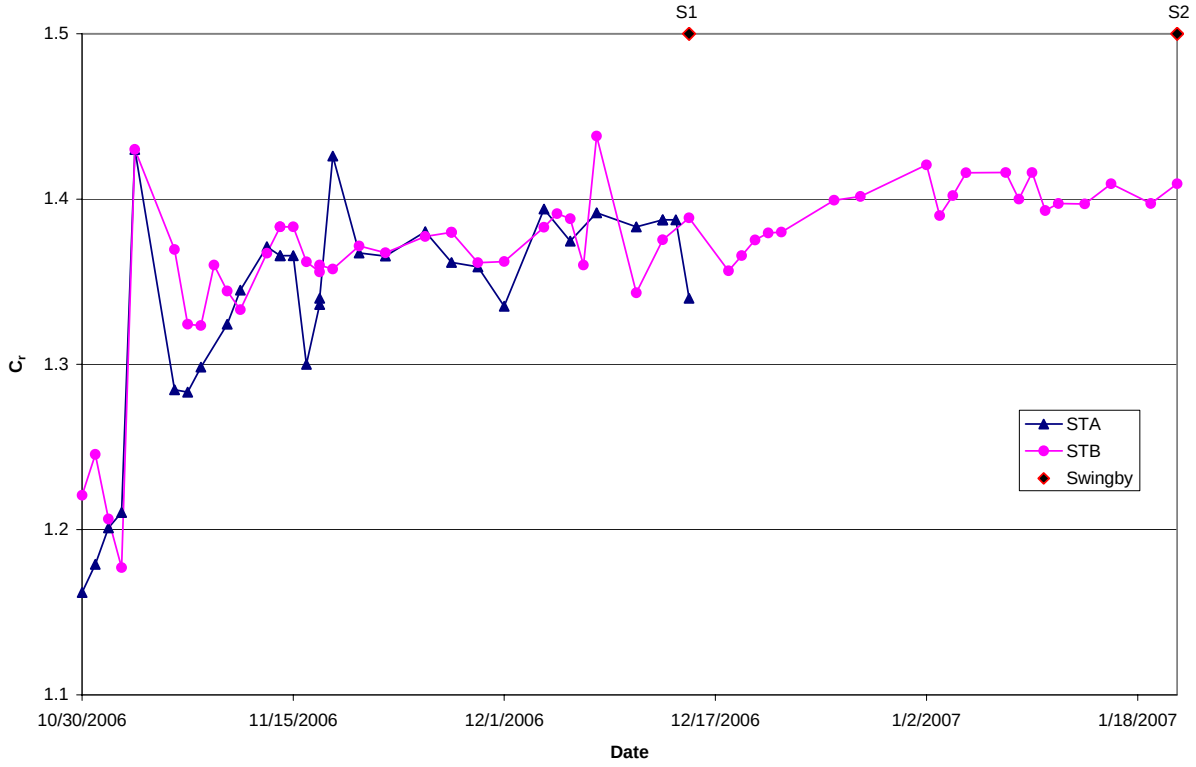

Figure 5. Estimated C_r Values for Ahead and Behind During the Phasing and Outer Loops

Comparisons with JPL Navigation Solutions

The JPL Multi-mission navigation team was funded to provide some independent orbit determination solutions at important times during operations. Orbit solutions were obtained and compared at "Separation plus 24 hours" and prior to perigees 1 and 4. Solution arcs were chosen and both centers used the same arc lengths with the same data. There are minor differences in terms of processing methods. Both centers used batch least-squares OD estimators. The JPL team routinely screens all tracking measurements below 10° in elevation[6] whereas the FDF navigation team routinely uses an elevation of 7° as well as editing of data measurements outside of a 3-sigma envelope.

Figure 6 below displays the parallel differences between definitive ephemerides determined at FDF and JPL for solutions generated with 24 hours of tracking data. As can be seen from the graph, the position differences between the two NASA centers were less than 700 meters, with an average total difference of 434 meters for Ahead and 286 meters for Behind. The FDF solution for Ahead was much more accurate than the FDF solution for Behind at this point based on orbital parameter estimation statistics and results, yet the comparison to JPL was higher than for Behind. The pre-mission error analysis (see Table 1) performed indicated that the expected FDF solutions will have orbital knowledge of 800 meters definitive. The parallel comparisons of the FDF solutions to the JPL Nav solutions are all within this uncertainty, a strong confirmation of the parallel results. Velocity comparisons are within 7 cm/s for both spacecraft with an average of 1.8 cm/s for Ahead and 0.5 cm/s for Behind.

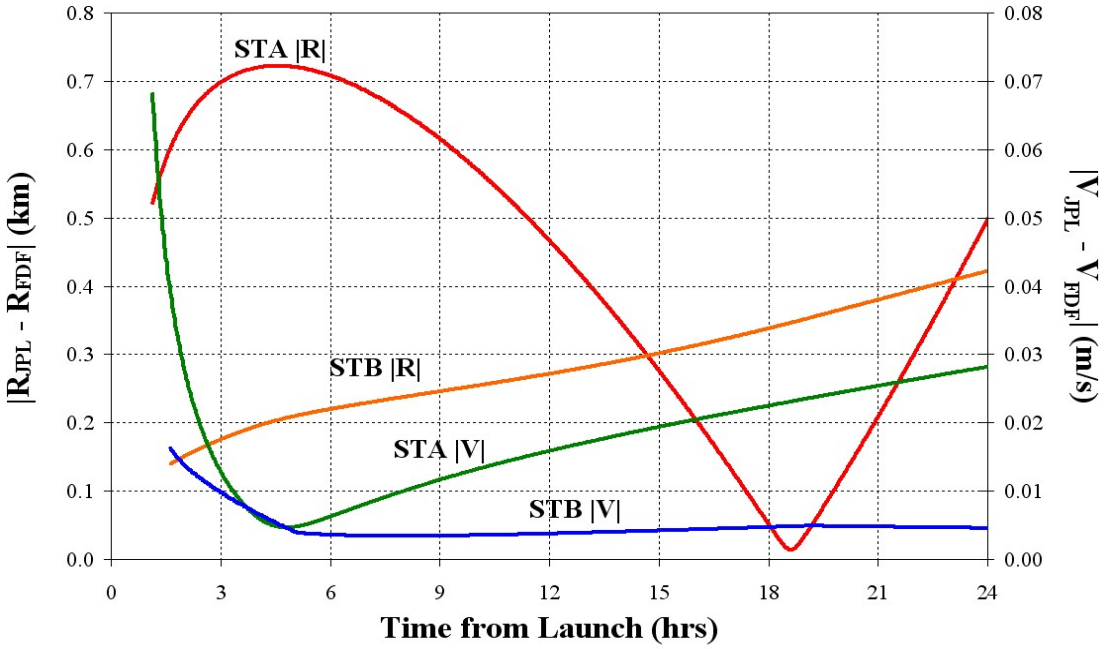

Figure 6. STEREO Parallel Definitive Ephemeris Compare Between FDF and JPL Solutions for First 24 Hour OD Solution Arcs

Figure 7 shows the parallel FDF-JPL OD results using tracking data from the first apogee, A1, to the first perigee, P1. The position differences between the two solutions were under 900 m during the data arcs with an average difference of 180 m for Ahead and 589 m for Behind. The primary contributor to the RMS position difference was the cross-track difference. The velocity differences between the two solutions were less than 4 mm/s.

[6] Tomas J. Martin-Mur, JPL Multi-Mission Navigation, meeting notes from FDF visit, June 2006.

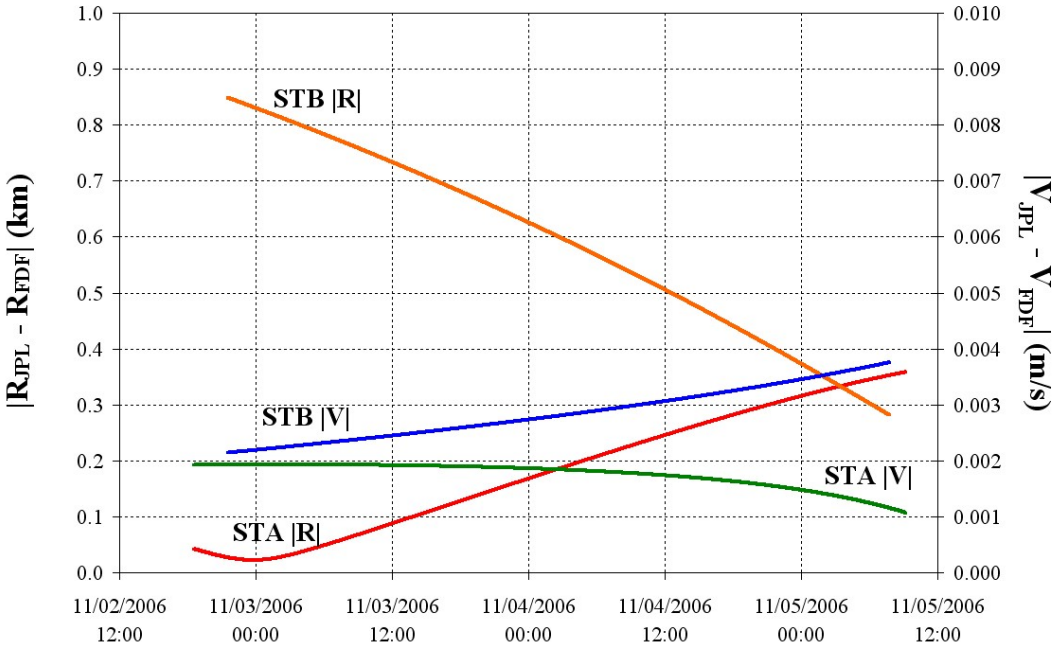

Figure 7. STEREO Parallel Definitive Ephemeris Compare Between FDF and JPL Solutions from A1 to P1

Figure 8 shows the parallel FDF-JPL OD results using tracking data from the fourth apogee, A4, to the fourth and final perigee, P4. The position differences between the two solutions were under 500 m during the data arcs with an average difference of 210 m for Ahead and 262 m for Behind. Again, the primary contributor to the RMS position difference was the cross-track difference. The velocity differences between the two solutions were less than 3 mm/s. These results are well within the mission requirements at final perigee (9.4 km and 2.7 cm/s).

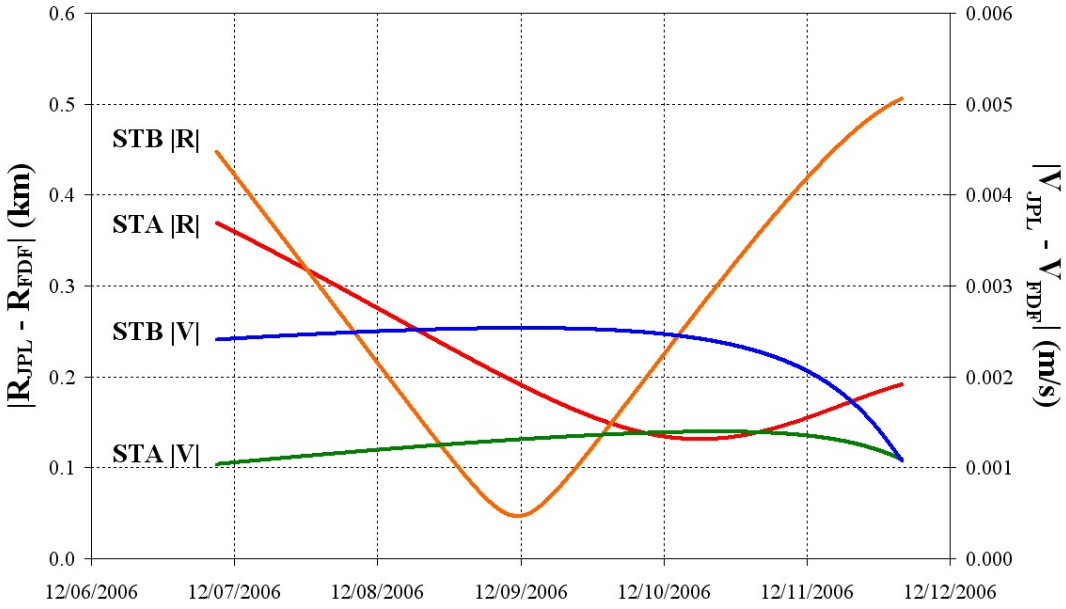

Figure 8. STEREO Parallel Definitive Ephemeris Compare Between FDF and JPL Solutions from A4 to P4

4. Conclusions

The addition of X-band capability for spacecraft ranging has permitted the GSFC FDF to expand its capabilities in support of orbital regimes for missions beyond the near Earth distances that utilize S-band electromagnetic spectrum frequencies for ranging support. The higher X-band frequencies are necessary for navigation support of the deep space regions that will figure largely in the future goals of NASA's Vision for Space Exploration. The STEREO spacecraft serve as a successful demonstration of this capability from the initial operations concept, through the specifications and implementation phase of this enhancement, testing, and actual on-orbit mission support.

Pre-mission error analysis studies of the expected accuracy levels achievable for STEREO are validated by the on-orbit navigation results of the FDF. The performance of the spacecraft was optimal, and the navigation results for

each phase of the mission have been as predicted. The FDF navigation results have been further validated by comparison of the FDF orbital solutions to the results of the JPL Multi-Mission Navigation Team. Confirmation of FDF results from three separate validation study periods for both Ahead and Behind was achieved.

The STEREO mission is also significant in that it has been a successful cooperative effort between multi-NASA centers with the prime mission design and operations team at APL, the navigation support from GSFC FDF, and the tracking support from JPL's DSN. All of the teams spent several years planning and preparing in concert for this mission, with each team's success dependent on the success of the others.

Members of the FDF STEREO support team wish to thank the APL STEREO Mission Team for the opportunity to share in this journey, in particular David Dunham, Peter Sharer, Jose Guzman, Daniel Ossing, and John Eichstedt. Also, the team wishes to acknowledge the assistance of Anne Long of a.i. solutions, Inc., as well as the members of the JPL Navigation team, for their time and valuable assistance with providing test data results and validation support of the STEREO orbital solutions.

5. References

1. Sharer, P., Driesman, A., Dunham, D., and Guzman, J., "STEREO Overview and History", AAS/AIAA Astrodynamics Specialist Conference, Mackinac Island, MI, August 19-23, 2007.

2. Ossing, D., Dunham, D., Guzman, J., Heyler, G., and Eichstedt, J., "STEREO First Orbit and Early Operations", AAS/AIAA Astrodynamics Specialist Conference, Mackinac Island, MI, August 19-23, 2007.

3. Dunham, D., Guzman, J., and Sharer, P., "STEREO Phasing Orbits", AAS/AIAA Astrodynamics Specialist Conference, Mackinac Island, MI, August 19-23, 2007.

4. Guzman, J., Dunham, D., Sharer, P., Hunt, J., Ray, J., Shapiro, H., Ossing, D., and Eichstedt, J., "STEREO Mission Design Implementation", 20th International Symposium on Space Flight Dynamics, Annapolis, MD, September 24-28, 2007.

5. Dunham, D., Guzman, J., Sharer, P., and Friesen, H., "STEREO Mission Design", Dunham, D., 20th International Symposium on Space Flight Dynamics, Annapolis, MD, September 24-28, 2007.

6. 820-013, Deep Space Mission System (DSMS) External Interface Specification JPL D-16765, *TRK 2-34 DSMS Tracking System Data Archival Format*, Original Release: April 30, 2000, Revision F: August 31, 2005

7. 810-005*, Rev. E. DSN Telecommunications Link Design Handbook, Module 203, Rev. A, Sequential Ranging,* Released February 20, 2006

8. T. Moyer, *Formulation for Observed and Computed Values of Deep Space Network Data Types for Navigation*, John Wiley and Sons 2003, Chapter 13.5.

9. C. Huang et al., "Relativistic Effects for Near-Earth Satellite Orbit Determination," *Celestial Mechanics and Dynamical Astronomy*, vol 48, 1990, pp. 167-185

10. D. McCarthy and G. Petit, *IERS Conventions (2003)*, IERS Technical Note No. 32

11. J. McCarthy et al., GEODYN II-Volume 1, System Description Volume 1, February 26, 1993